

## Electronic Supplementary Information

# The Thin Carbon Layer Coated $\text{Ti}^{3+}$ - $\text{TiO}_2$ Nanocrystalline for Visible-Light Driven Photocatalysis

Baojiang Jiang,<sup>a</sup> Yunqi Tang,<sup>a</sup> Yang Qu,<sup>a</sup> Jian-Qiang Wang,<sup>b</sup> Ying Xie,<sup>a</sup> Chungui Tian,<sup>a</sup> Wei Zhou,<sup>a</sup> Honggang Fu<sup>\*a</sup>

<sup>a</sup> Key Laboratory of Functional Inorganic Material Chemistry, Ministry of Education of the People's Republic of China, Heilongjiang University, Harbin 150080, China;

<sup>b</sup> Shanghai Synchrotron Radiation Facility (SSRF), Shanghai Institute of Applied Physics, Chinese Academy of Sciences, Shanghai, China

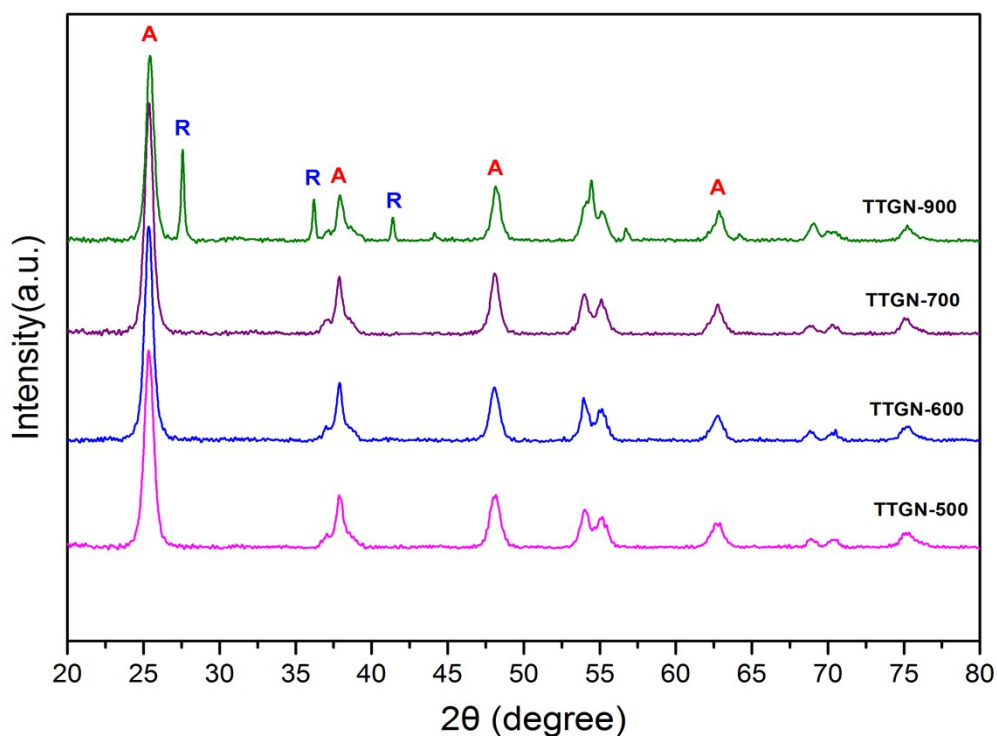


**Figure S1.** XRD patterns of many products by calcinations for different time under nitrogen. Standard diffraction peaks of anatase  $\text{TiO}_2$  and rutile  $\text{TiO}_2$  are marked by “A” and “R”, respectively.

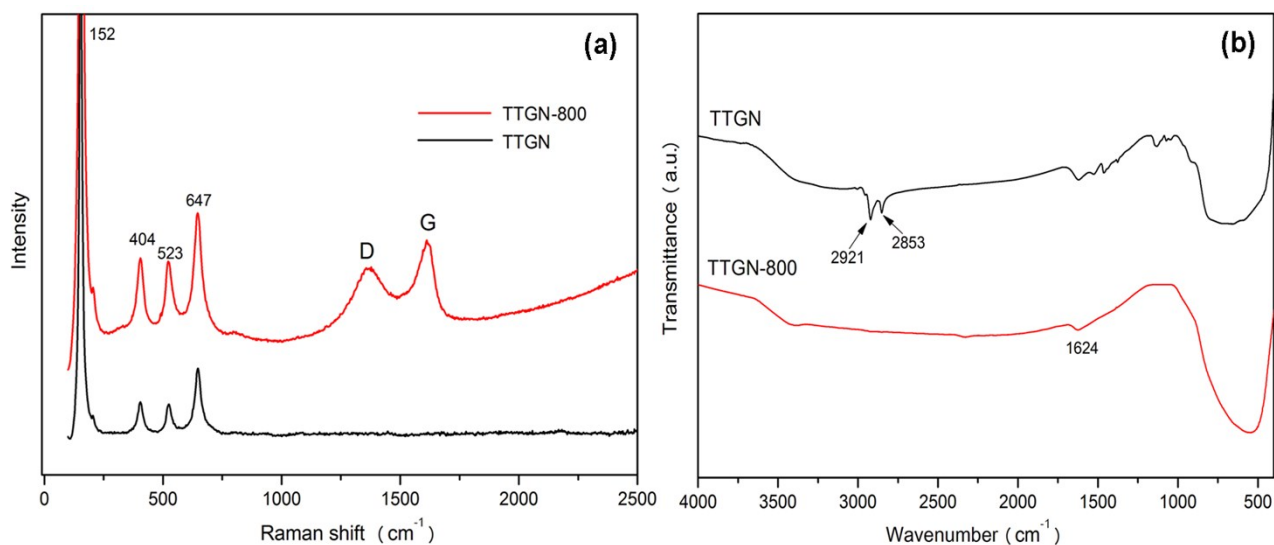


**Figure S2.** (a) Raman spectra of TTGN and TTGN-800, the D band and the G band are assigned to the carbon shell in composites. (b) FT-IR spectra of different samples including TTGN and TTGN-800 via programmed calcination approach at 800 °C.

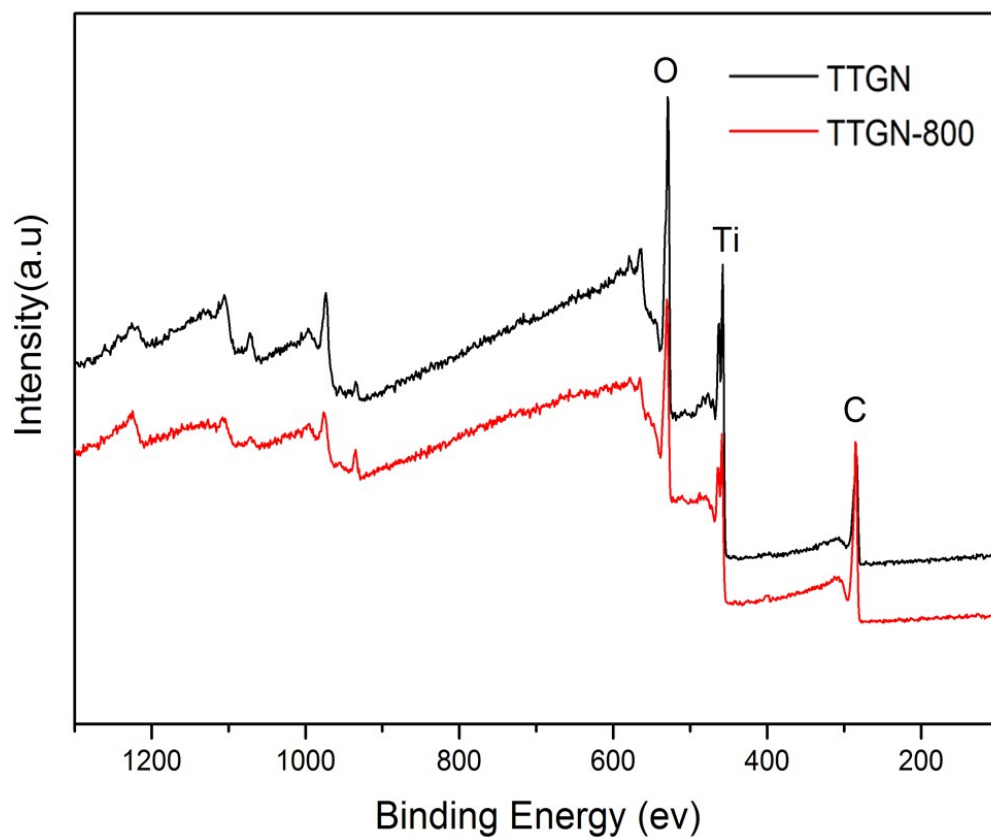


**Figure S3.** The XPS wide spectra for different sample.

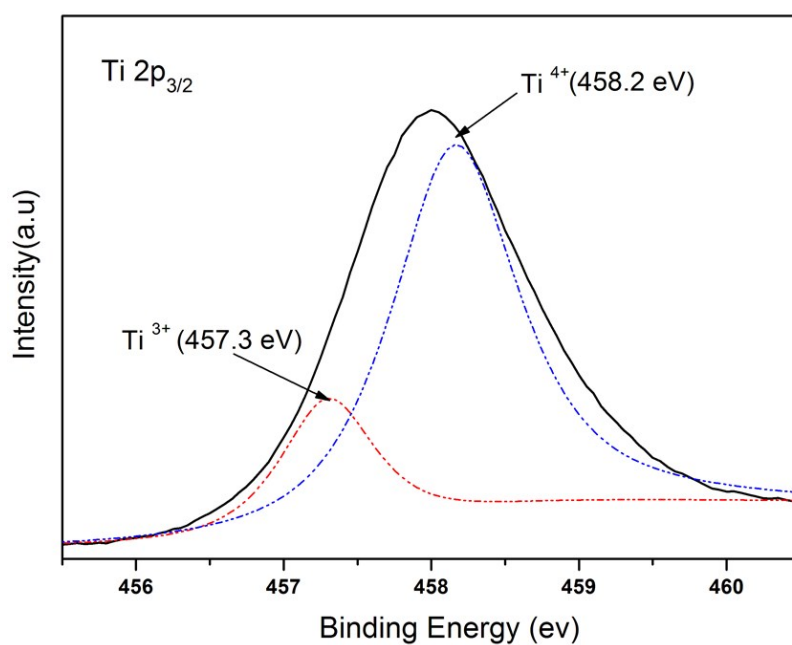


**Figure S4.** The Ti 2p<sub>3/2</sub> XPS spectra of TTGN-800.

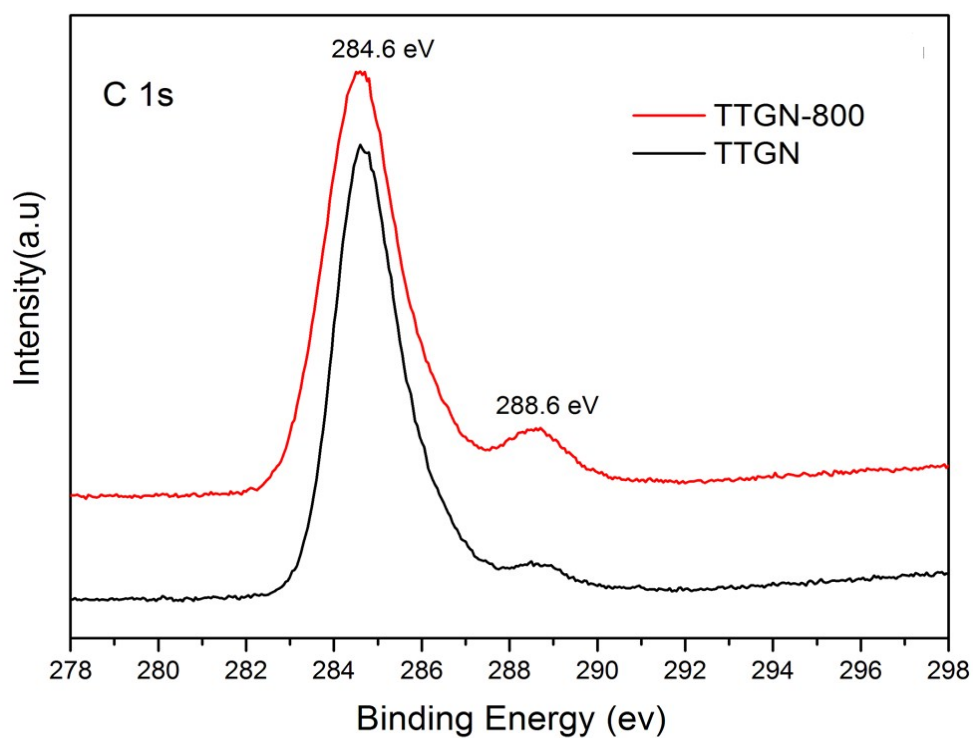


**Figure S5.** The high-resolution C1s XPS spectra of TTGN and TTGN-800.

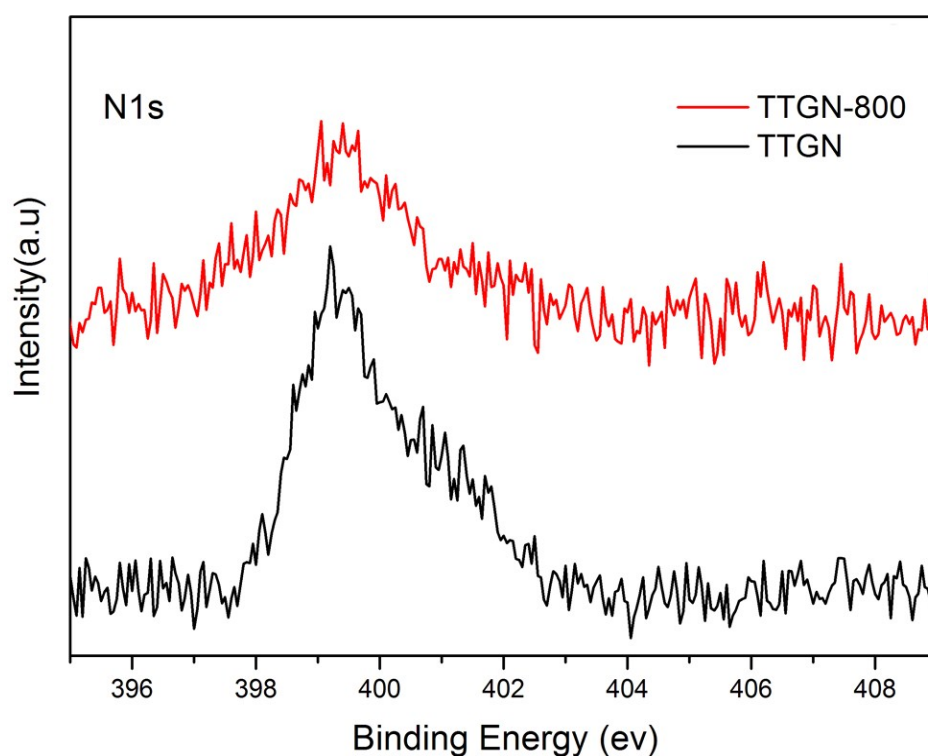


**Figure S6.** High-resolution N1s spectra of TTGN and TTGN-800, respectively.

The main C 1s peak for TTGN shows the presence of C-C and C(O)O chemical binding states, corresponding to the peak at 284.6 and 288.6 eV, respectively (Figure S4). After the thermal

treatment process, the peaks of C(O)O become strong. All these results can further confirm the successful incorporation of titania and carbon. It is noted that Figure S5 show the N1s peaks of TTGN and TTGN-800. The presence of nitrogen peak in TTGN implies the incorporation of nitrogen atoms within the composites, and the doping level is about 1.95 % (atom ratio). As a result, the atomic percentage of nitrogen is also decreased to 1.35 % after high temperature calcinations at 800 °C under nitrogen, indicating the most part of N species modifies the surface of products by active group interaction. This tendency is very similar to the previous results, further confirming that the nitrogen modifying is easily achieved in our work. The presence of N element not only affects the separation and the migration of photo-generated charge carriers, but also possibly enhances the adsorption ability photocatalysts for the atrazine and MB.

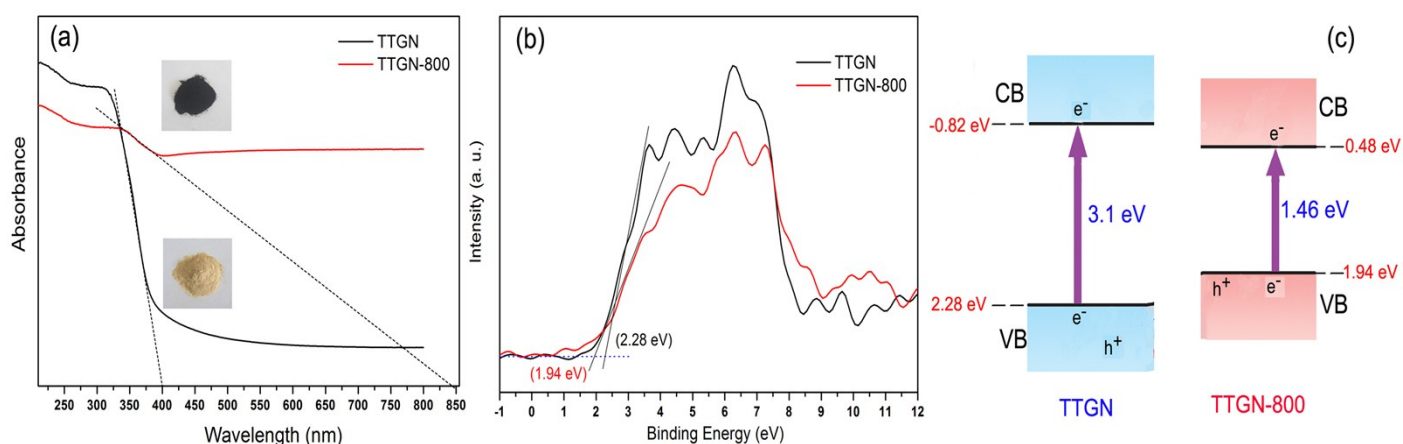


**Figure S7.** (a) UV-vis diffuse reflectance spectroscopy, (b) Normalized XPS valence band spectra, and (c) scheme for the energy band structure of TTGN and TTGN-800.

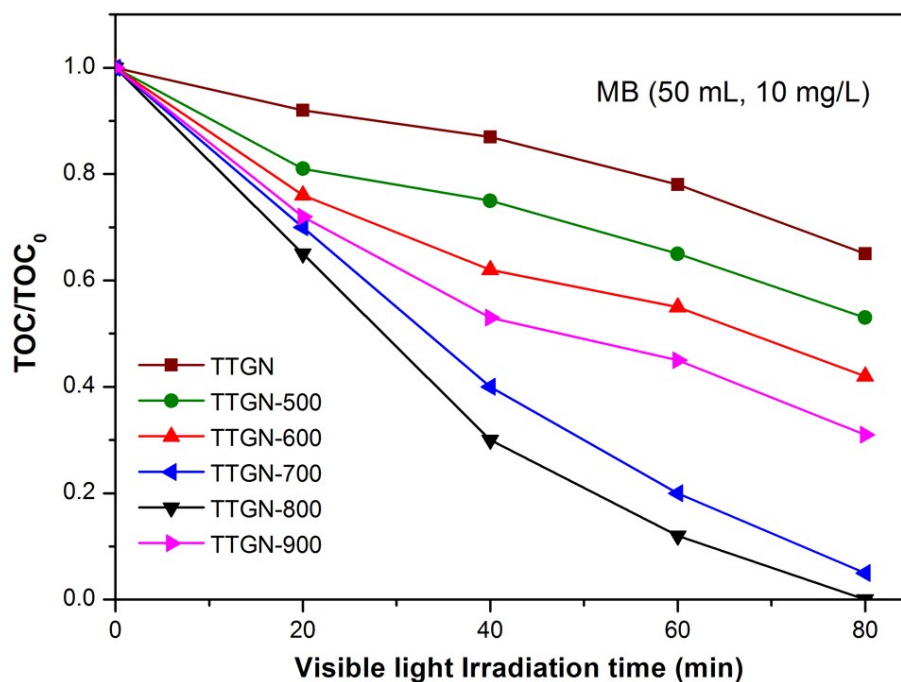


**Figure 8.** Time profiles of photocatalytic degradation of MB for different catalysts under visible light irradiation. The TOC and  $TOC_0$  are the reaction concentration and the initial concentration of MB solution, respectively.

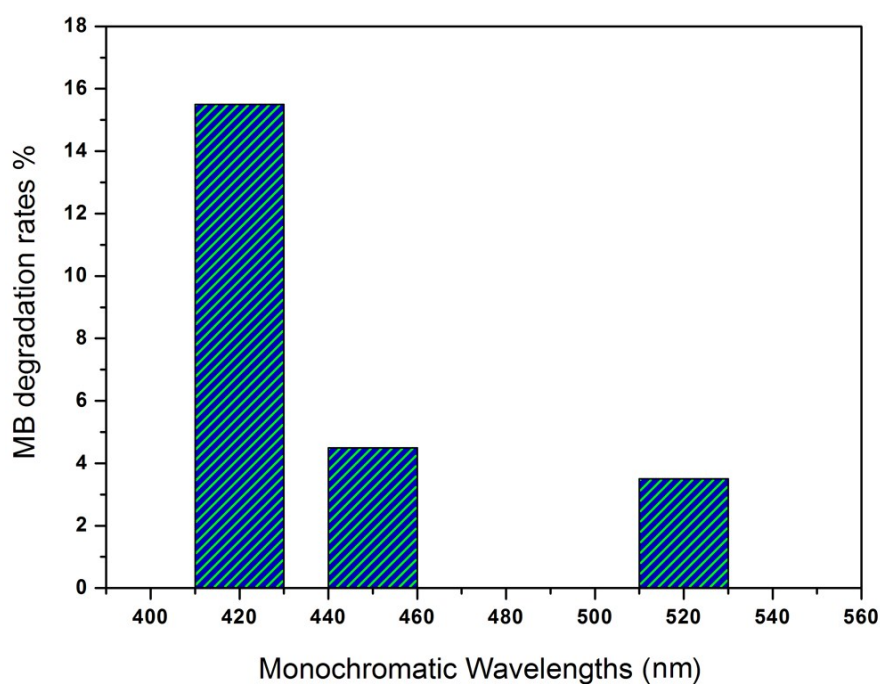


**Figure 9.** Wavelength dependence of MB decomposition by the TTGN-800 upon illumination of monochromatic lights with various wavelengths (420, 450, 520 nm) for 60 min. These monochromatic lights generated using different band pass filters have nearly identical intensities ( $10 \text{ mW cm}^{-2}$ ).

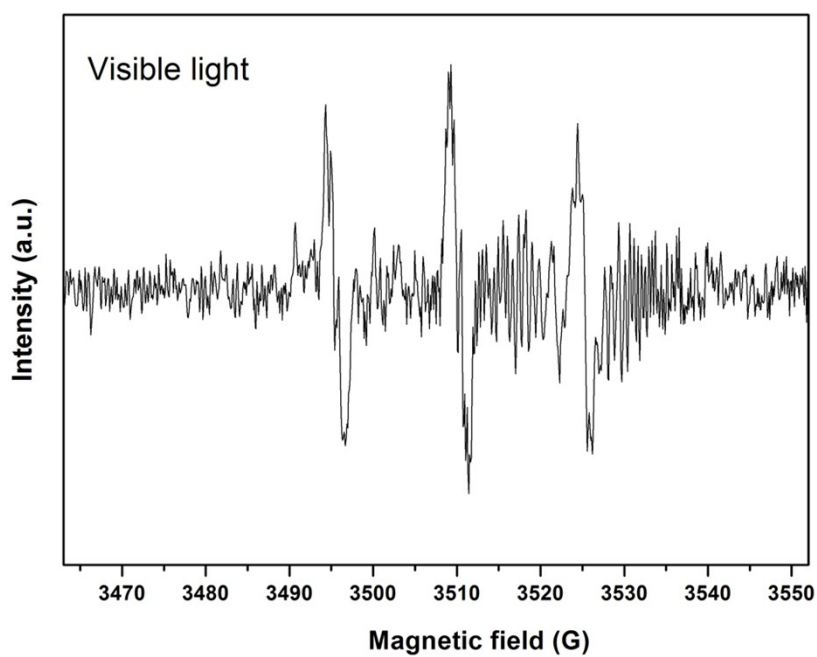


**Figure S10.** The PBN spin-trapping ESR spectra of the typical sample TTGN-800 in saturated aqueous after 5 min visible light irradiation. Catalyst loading (TTGN-800): 1g/L; PBN concentration: 0.01mol/L.